CMMoST 2021

6TH INTERNATIONAL CONFERENCE ON

Mechanical Models in Structural Engineering

01 – 03 December 2021

Escuela de Ingenierías Industriales
Universidad de Valladolid

Full Papers

UNIVERSIDAD DE GRANADA

UNIVERSIDAD D SEVILLA

Universidad de Valladolid

6^{th} International Conference on Mechanical Models in Structural Engineering

CMMOST 2021

Valladolid, December 2021

Editors

Antolín Lorenzana Ibán

Luisa María Gil Martín

Enrique Hernández Montes

Margarita Cámara Pérez

Víctor Compán Cardiel

Andrés Sáez Pérez

Coordination and design

Álvaro Magdaleno González

Escuela de Ingenierías Industriales. Universidad de Valladolid
Paseo del Cauce 59, 47009 Valladolid (Spain)
cmmost21@uva.es

ISBN: 978-84-09-39323-7

SPONSORS


ITAP


Ayuntamiento de
Valladolid


MICHELIN


CARTIF


Spanish Group
IABSE


media madera
ingenieros consultores


Colegio Oficial de
Ingenieros Industriales
de Madrid


acoustic
camera

CONTENTS

Evaluation of vibration transmission of L-shaped plates using finite element analysis

Jesús Magdaleno[1], Enrique Segovia[2], Jesús Carbajo[3], Jaime Ramis[4], M. Ángeles Martín[5]

ABSTRACT

In this paper, velocity level difference through L-shaped plates is studied using finite element analysis (FEA). Validation is performed using experimental measurements and comparing different finite elements models. The velocity level difference between the source and receiving plate is used to study how vibration flows for third-octave frequency bands, within the frequency range 40-3150 Hz. The influence of different types of geometry, material properties, meshes, types of excitations and the incorporation of an elastic layer, simulating a floating floor, were studied. The use of finite elements models with 2D elements proved to be adequate and a good approximation was obtained from both experimental and finite element analysis results.

Keywords: L-shaped plates, vibroacoustic, finite element analysis, vibration.

1. INTRODUCTION

The study of vibration transmission and energy flow between coupled plates improves the predictive models of structure-borne sound transmission. This is of interest in many fields of application, e.g., in automotive, aeronautic, marine, and building industries [1].

The Finite Element Method (FEM) is increasingly used to build predictive models. It is also used to validate analytical and numerical methods, although verification and validation of FEM models are necessary [2]. This is not sufficiently documented in many cases.

Simmons [3] used FEM to calculate the vibrational energies of plates forming L- and H-structures at discrete frequencies between 10 and 2000 Hz, where one plate is excited by a point force and power is transmitted through the junction to other plates. The kinetic energy on a plate was derived from the measured or the calculated displacements at n evenly distributed points to compare experimental, FEM and SEA (Statistical Energy Analysis) results. The FEM gave very good estimates in general.

An analytical model of the bending wave transmission between semi-infinite thin plates connected by a hinge or by an elastic interlayer is studied in [4], with different elastic interlayers in a T–junction. In

[1] *School of Industrial Engineering, University of Valladolid (SPAIN). magdal@uva.es (Corresponding author).*
[2] *Department of Physics, System Engineering and Signal Theory, University of Alicante (SPAIN).*
[3] *Research Institute for Integrated Coastal Zone Management-IGIC, Polytechnic University of Valencia (SPAIN).*
[4] *Department of Physics, System Engineering and Signal Theory, University of Alicante (SPAIN). jramis@ua.es.*
[5] *School of Industrial Engineering, University of Valladolid (SPAIN).*

this work, a two-dimensional finite element model is used to calculate a correction factor for stiffness. Steel and Craik [5] used a finite element model to overcome SEA limitations at low frequencies and study the coupling loss factor (CLF) for walls in buildings more accurately. In [6] the FEM is combined with a Statistical Energy Analysis-like (SEAL) for derivation of energy flow between two thin plates. A thin L-shaped plate is investigated using a commercial FE code. Mace and Shorter [7] used energy flow models from finite element analysis, with harmonic excitation, in a system comprising three coupled plates. Traditional SEA predictions were inaccurate in this case. In [8], a power flow density vector of L-shaped plates is used adopting a substructure approach, comparing results with those obtained with the FEM. Hopkins [9] [10] studied an L-junction and a T-junction, with agreement between both FEM and data measured with SEA at high frequencies. Monte Carlo methods were used to evaluate the uncertainty in the material properties and dimensions. Results from the numerical experiments are used for calculating the change in the coupling parameters and their use in SEA and the vibration reduction index in European standard EN 12354 [11].

A benchmarking exercise is presented in [12] for SEA analysis of semi-infinite, isotropic, thin and flat plates. The transmission coefficient is determined by considering a wave to be incident on the junction formed by the intersection of several semi-infinite plates. To facilitate exactitude assessment and help to boost the designer's confidence in simulation, Bochniak and Cieslik [13] introduced uncertainty considerations in vibration energy flow analysis. They used the structural intensity pattern, which presents a vectorial nature of vibrational energy flow in structures, and FEM was used for obtaining harmonic response solution. In [14] the verification of the results obtained was performed on FEM and genetic algorithms were applied to the evaluation of the fundamental frequency of stiffened plates.

Clasen and Langer [15] analysed the influence of various damping mechanisms on the transmission of sound in buildings, using FEM models, studying different constructive configurations. They analysed the influence of damping on the joints of walls, introducing a spring-damper system in several small-scale models. Du et al. [16] studied uniform elastic boundary restraints in two elastically coupled rectangular plates with an analytical method, validating the results with FEM models. The FEM is used in [17] to obtain a numerical evaluation of the vibration reduction index in structural joints, comparing results with those evaluated using the EN 12354 [11], and allowing the calculation of an adaptation term that makes both approaches converge. Comparison with results obtained by empirical formulas reveals that results from the standard's calculation cannot accurately reproduce the expected behaviour, and thus indicate that alternative complementary calculation procedures are required. The behaviour of a structural joint in terms of vibration transmission is complex, depends strongly on the frequency, and should be evaluated for each structural reality. The prediction of vibration transmission across networks of coupled beams using a bending wave only model and a bending and longitudinal wave model is studied in [18], by application of SEA and advanced SEA to structure-borne sound transmission. SEA is used with coupling loss factors determined from wave theory and is compared with numerical experiments from FEM. 2D and 3D FEM models of an acoustic laboratory were used in [19], and the results were verified with experimental measurements, to study airborne sound properties of composite structural insulated panels. The 2D results obtained a good agreement with experimental results.

In [20] the vibration problems of various types of coupled plates are solved using an improved Fourier series method. The method was validated with results obtained by the finite element analysis. In addition, numerical results (FEM) are presented in [21] to validate the correctness of an improved Fourier series method used to analyse the vibration of moderately thick coupled rectangular plates with general elastic boundary supports and arbitrary coupling conditions.

Poblet-Puig and Guigou-Carter [22] used spectral finite elements for parametric analysis of the vibration reduction index of heavy junctions oriented to flanking transmissions and EN-12354 prediction method. A parametric analysis of the vibration reduction index was performed for several junction types, observing the influence of several parameters such as damping, junction dimensions and the mass ratio. Hopkins et al. [23] also used the vibration reduction index and developed new regression curves by numerical experiments with FEM, SFEM and wave theory. The junctions considered were formed from heavyweight walls and floors and the new relationships were implemented in the prediction models improving the agreement between the measured and predicted airborne and impact sound insulation.

One of the difficulties that arise when computational methods are used is the need for methods to evaluate the reliability and accuracy of their results. In the field of FEM application in the transmission of sound in buildings, this fact was evidenced by [2]. They indicate that the reliability of the FEM depends heavily on the way the model is defined and include validation through experimental measures in a study of low-frequency dwellings.

In one of the first works on FEM application in structural sound transmission, Simmons [3] points towards the need to verify that the commercial program used produces valid results, since there are no published previous cases of usage in the frequency range of interest. To do this, he compares simple cases for which the analytical solution is known, or for which experimental results exist, with the results of the program. Concerning the dynamic analyses, Wilson [24] indicates that to reduce errors caused by model approximations, many different analyses are necessary, and unsurprisingly there are 20 of them. In each analysis, different calculation models, loadings and/or boundary conditions are used.

Verification and validation are the main methods and procedures used to assess reliability, limitations, weaknesses, and uncertainties of computational simulations. In [25] examples are found of typical situations in which errors are commented and techniques are proposed for verifying and validating. A more detailed process can be found in [26], [27] and [28].

The accuracy in FEM depends on the size of the mesh, element quality, etc. In [29] a smoothed finite-element/boundary-element coupling procedure (SFEM/BEM) is extended to analyse the structural-acoustic problem to improve accuracy.

In this paper we aim at analysing the vibroacoustic response obtained by FEM models in the case of L-linked plates, using the commercial FE package I-DEAS. The difference in velocity level between the excited element and the non-excited element, $D_{\mathrm{v,ij}}$, will be used as an indicator of vibration transmission. This parameter is also used by other authors [9] [1] [22]. The experimental model will be made using stone with concrete-like properties. The influence of the thickness of the connected plates, different characteristics of the material, meshes and the incorporation of two samples of

elastic layers, similar to floating floors, will be studied. The results will be validated and calibrated using experimental measures and comparing different FEM calculation models. Third-octave frequency bands within the frequency range 40-3150 Hz will be studied.

2. METHODOLOGICAL APPROACH

2.1. Background theory

Vibration transmission at junctions where building elements connect is related to the vibration reduction index (K_{ij}), [30] [31] [11], and is normalized to obtain invariant magnitude.

$$K_{\mathrm{ij}} = \frac{D_{\mathrm{v,ij}} + D_{\mathrm{v,ji}}}{2} + 10\log\frac{L_{\mathrm{ij}}}{\sqrt{a_{\mathrm{i}} a_{\mathrm{j}}}} \tag{1}$$

where $D_{\mathrm{v,ij}}$ is the velocity level difference between source element i and receiver element j, L_{ij} is the junction length between elements i and j, and a_i is the equivalent absorption length given by

$$a_{\mathrm{i}} = \frac{2{,}2\,\pi^2\,S_{\mathrm{i}}}{c_o\;T_{\mathrm{s,i}}}\sqrt{\frac{f_{ref}}{f}} \tag{2}$$

in which S_{i} is the area, c_o is the speed of sound in air, $T_{\mathrm{s,i}}$ is the structural reverberation time, f_{ref} is a reference frequency (f_{ref} =1000 Hz) and f is the frequency.

This vibration transmission model is based on a simplified SEA theory of power transmission, where only bending waves are taken into consideration, and the number of subsystems considered are reduced to first order transmissions only [32]. In [32] [33] [34] [35] a review of prediction models, included in building acoustics regulations, can be found along with the advances that have been made and detected needs for improvement. It is possible to obtain the value of K_{ij} using velocity level measurements (L_{v}), as well as the structural reverberation time (T_{s}) of the two elements [31].

Initially, the parameter to be determined based on the velocities is the average velocity level L_{v}. For stationary, structural or aerial excitation, the spatial average is calculated using

$$L_{\mathrm{v}} = 10 \cdot \log\frac{v_1^2 + v_2^2 + \cdots + v_n^2}{n \cdot v_0^2} \quad dB \tag{3}$$

where $v_1^2 + v_2^2 + \cdots + v_n^2$ are the mean square velocities at n different positions on the element, in m/s, and v_0 the reference velocity ($v_0 = 1 \times 10^9$ m/s). As from L_{v} the difference in velocity level $D_{\mathrm{v,ij}}$ is determined using

$$D_{\mathrm{v,ij}} = L_{\mathrm{v,i}} - L_{\mathrm{v,j}} \tag{4}$$

The comparison between the experimental measurements and the FEM models will be done by means of $D_{\mathrm{v,ij}}$, to avoid the influence of structural reverberation time on the calculations. This parameter is also used by other authors [9] [1] [22]. Energy measurement by using velocity measurement points is used in [36] [37], where the number and position of these points are chosen at random and without any precise criterion. This type of approach gives satisfactory results for high

frequencies, but large variations appear at low frequencies. It is not intended to compare the results with those predicted by the SEA, but a similar methodology is used.

2.2. Experimental study

Two cases of perpendicular plate joints were studied. The first joint was formed by two thick plates with a thickness of 60 mm and dimensions of 560 × 530 mm for the horizontal plate and 640 × 530 mm for the vertical plate (Fig. 1). The second joint consisted of a thick horizontal plate with a thickness of 60 mm and dimensions of 545 × 530 mm and another thin vertical plate with a thickness of 30 mm and dimensions of 640 × 530 mm. All measurements had a tolerance range of ± 1 mm. Washers were attached every 50 mm following a matrix pattern to facilitate data collection (Fig. 1). The response was measured in each of the washers.

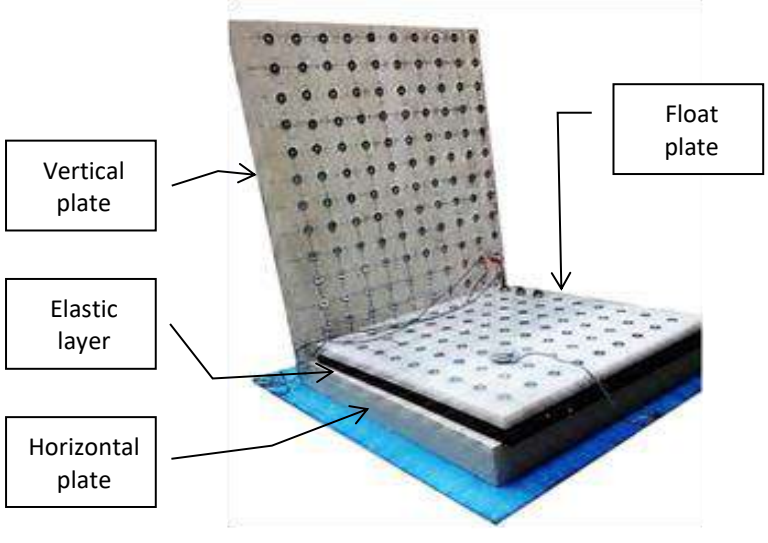

Figure 1. *Geometry of the joint connecting thick plates and floating plate.*

Material used for the plates was a type of stone, called Bateig. Its physical properties are similar to those of concrete, and are described in *Table 1* [38]. Some of the properties of the material were used to calibrate FEM analysis results.

Table 1. Nominal properties of Bateig stone (Bateig32).

Young's modulus (E)	32 GPa
Poisson's ratio (ν)	0.23
Density (ρ)	2315 Kg/m^3
Structural damping coefficient	0.01
Sound speed (c)	3718 m/s

In the study that included an elastic layer, a marble plate was used as a floating plate, with a thickness of 20 mm, a density of 2656 kg/m3, a Young's modulus of 80 GPa and a Poisson's ratio of 0.3. The properties of the elastic layers are detailed in *Table 2*.

Experimental measurements were made by placing the sample on a material that allowed movements from the supporting surface (Fig. 1). The excitation was produced by an electrodynamic type of

actuator, similar to that used in Distributed Mode Loudspeakers (DML). The input signal was a Maximum Length Sequence (MLS) [39]. An NI PCI-6120 data acquisition card was used. The excitation occurred in the same three points as the FEM model (Fig. 3a).

Table 2. Properties of the elastic layers.

Elastic layer	Thickness mm	Density (ρ) Kg/m^3	Dynamic stiffness (s') MN/m^3	Structural damping coefficient
Elastic layer 1	12.5	697.63	5.34	0.17
Elastic layer 2	30	94.83	13.93	0.077

The measurement was carried out simultaneously at three different points, with three accelerometers. The measure points corresponded to the washers attached to the surface (Fig. 1). There were 81 points in the excited horizontal plate and 108 points in the unexcited vertical plate. Signals were registered using the LabWIEW platform with a sampling rate of 96 kS/s and processed using MATLAB.

2.3. FEM model

FEM models with 2D elements were used and the average surface of the plates was taken as reference. These plates were meshed with 8-node shell elements, called "Thin Shell - Parabolic Quadrilateral", with six degrees of freedom per node (three translational and three rotational). This element was based on Mindlin's thick plate equations, which included movement due to shear stress. The formulation is described in [40] [41]. The maximum element size used was 50 mm, so at least 33 elements per wavelength were used for the maximum frequency of interest in this study (2250 Hz). Specifications of meshes used in the models without elastic layers are detailed in *Table 3*.

Table 3. FEM mesh without elastic layer used in the numerical simulations.

	Model	
	Coarse mesh	Fine mesh
Element size (mm)	50	25
Number of Elements	264	1008
Number of Nodes	863	3163

To model the elastic layer of the floating floors, spring-type elements were used (Fig. 2). These elements were massless, translational node to node, and with structural damping coefficient. Spring stiffness was calculated based on the dynamic stiffness of the elastic layer, multiplied by the surface of the elastic layer and divided by the number of springs [42]. For the coarse mesh, 408 springs had a rigidity of 9590 N/m for elastic layer 1 and a stiffness of 3675 N/m for elastic layer 2.

In accordance with the experimental measurements and calculations made of own frequencies, an unconstrained system was used as the most appropriate model, with no movement restriction.

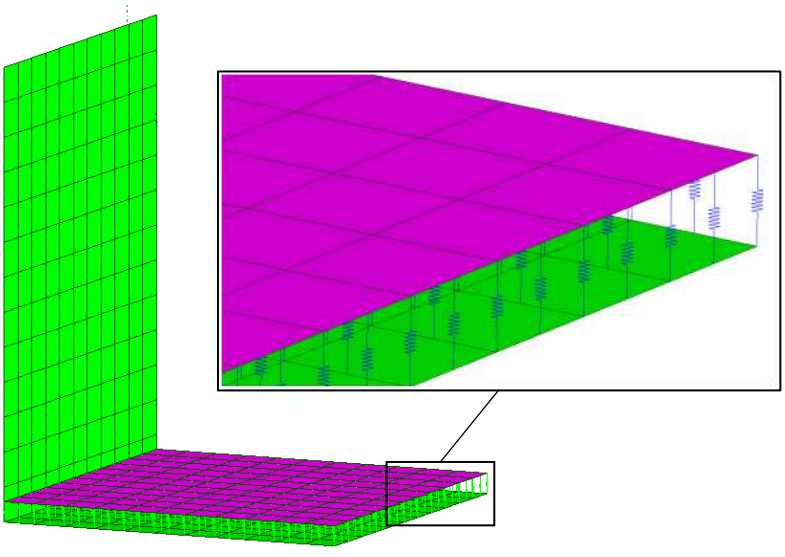

Figure 2. *Models with elastic layer. Mesh for the plates and for the elastic layer.*

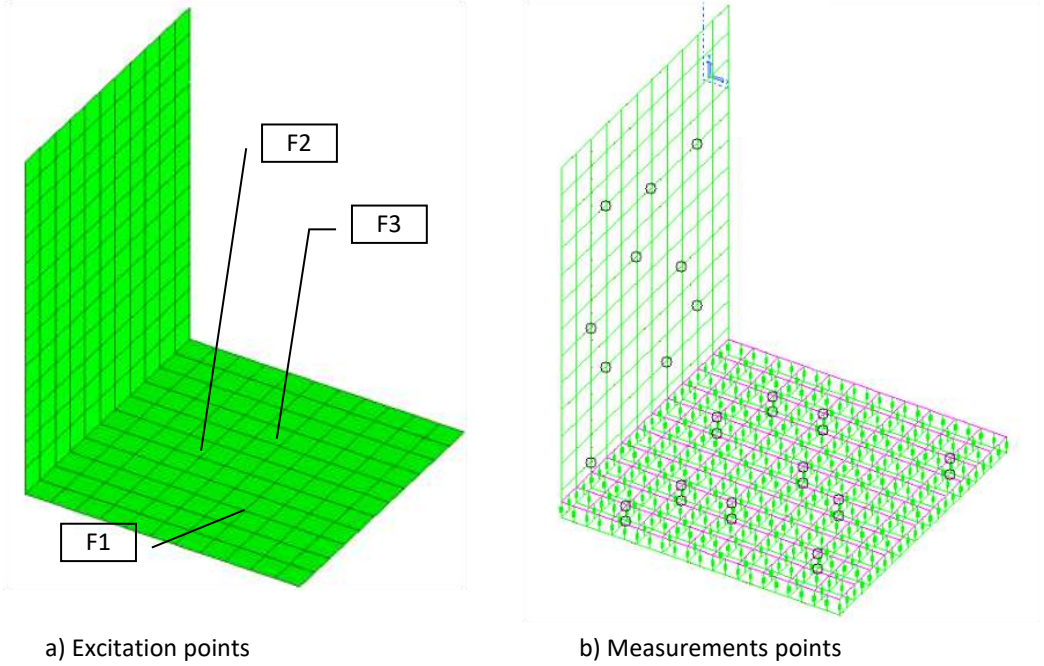

a) Excitation points b) Measurements points

Figure 3. *Excitation and measurements points in FEM models.*

Two types of excitations were used in the FEM models to analyse which of them best simulates the experimental method. The first type simulates transient excitation through a perpendicular impact to the surface, recording the response for 5 s in the models without an elastic layer and 10 s in models with the elastic layer, because of longer system response duration. The impact characteristics were determined so that the response had a similar amplitude to that obtained in the experiments. The second type of excitation simulated a stationary excitation by a series of impacts at a given point, with a frequency of 10 Hz, simulating a tapping machine (TM) [43]. The responses of both types of

excitations were calculated when applied to three points at similar positions to those used experimentally (Fig. 3a).

Since our objective was to determine velocities at different points, a modal analysis was made to determine own frequencies and own modes. Using the modal overlapping method, the response to the excitation was evaluated. Subsequently, the velocities obtained were processed to calculate speed levels and speed level differences.

3. VALIDATION AND CALIBRATION

FEM models must be validated and calibrated to obtain more reliable and accurate results. To do so, we evaluated the differences between several models, in addition to the differences with the experimental measures. The models of plates without elastic layers, i.e., without a floating plate, were validated and calibrated first. To do this, the results of own frequencies, average quadratic velocity, speed level and speed level difference were used. To start with, results obtained with the excitation at one point were used and the results with the excitations in other points were compared later to evaluate the predictive capacity of the model. We also evaluated the use of 10 velocity measurement points, instead of the dot matrix that was used in the experimental measurements. Some of the material's properties were used to calibrate the results of FEM analyses [44] [45]. For this, modifications in Young's modulus and in the density of the material were studied.

In the case of thick plate junction, mean square velocity results of the excited plate of the fine and coarse mesh models using a Young's modulus of 25 MPa show similar results to the experimental ones (Fig. 4). Therefore, this value of the Young's modulus and the coarse mesh seemed to be adequate for this case. The results of the mean square velocity in the FEM models, taking 10 velocity measurement points (Fig. 3b), were similar to those obtained using the same measurement points as those used in the experimental process (Fig. 4). Furthermore, speed level results differed by less than 2 dB from the 630 Hz band, when 10 measurement points were used, differences being somewhat greater at lower frequencies. Taking advantage of these similar results, the following analyses will use 10 velocity measurement points in FEM models, unless otherwise indicated.

Regarding the influence of the number of elements in FEM models, the maximum difference in own frequencies was 1.65% in mode 42 (3479 Hz), with differences smaller than 0.8% below 1753 Hz (mode 16). As for the differences between the experimental model and the FEM models, the maximum difference was 4.2%. The results on velocity levels in FEM models of thick plate junctions without elastic layer differed by less than 3 dB in most cases, having a similar frequency distribution in both plates, so a smaller difference was expected when the speed difference between plates was evaluated. Therefore, this confirmed the coarse mesh appeared to be of sufficient size and a more detailed convergence analysis was not considered necessary, although calculations were also performed for the thin mesh to check the effect of number of elements in the speed level difference.

An additional check was done based on the results of the speed level difference between the excited plate and the non-excited plate, to obtain an estimate of energy transmission. The response was related to similar frequency in the experimental results and in the FEM models (Fig. 5). Values of the FEM models were quite close to each other, at approximately 1 dB. Differences between the FEM models and the experimental results were around 4 dB.

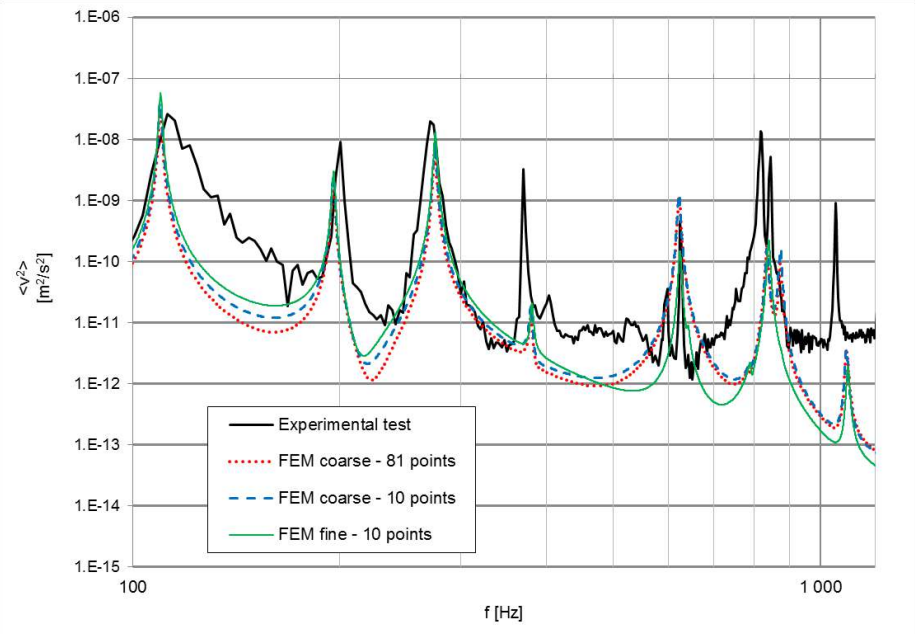

Figure 4. *Mean square velocity in the horizontal plate of the joint with thick plates without elastic layer. E=25 MPa. (<v²> - mean square velocity, f - frequency).*

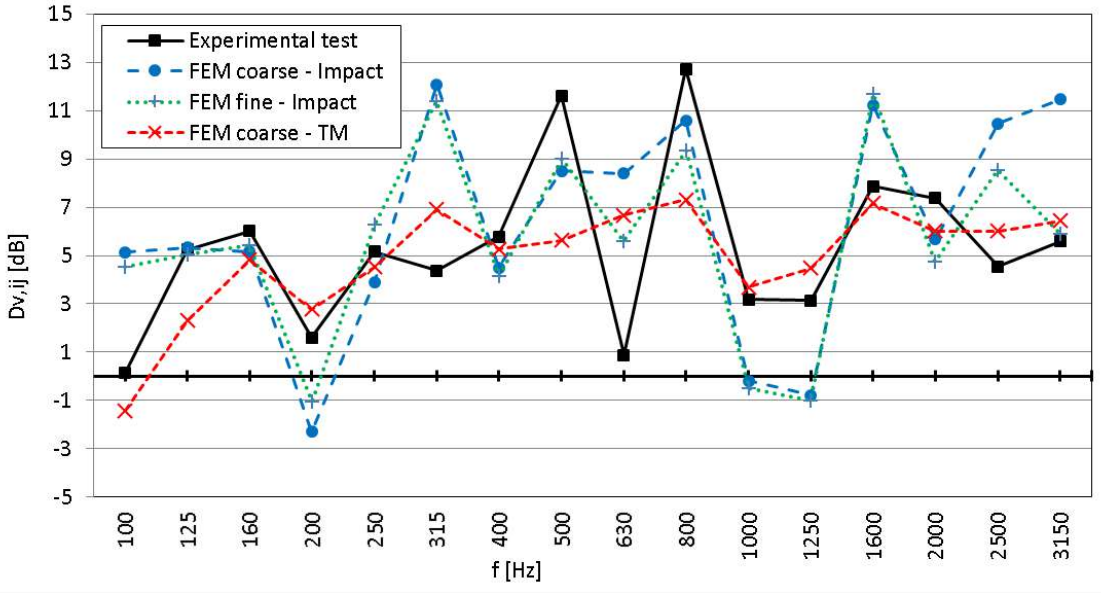

Figure 5. *Velocity level difference at the junction of thick plates with an elastic layer. Different meshes and excitation types ($D_{v,ij}$ - velocity level difference, f - frequency).*

The precision obtained seems acceptable compared to other studies. For example, [46] found standard deviations in Dv, between 2 dB and 10 dB in masonry walls, with an average of around 4 dB. These differences were greater at low frequencies.

To evaluate the predictive capacity of the model, responses of the thick plate model with excitations at other points were analysed, and a similar response was observed. A quantitative assessment will be given later when the results are presented.

Based on these studies, we can consider that the coarse mesh FEM model, material with E = 25 MPa and 10 points measures, achieved an accuracy that was adequate to describe junction behaviour of two thick plates without an elastic layer. Following a similar procedure, the most suitable model for thick plate-thin plate junctions, was the one using coarse mesh, material with E = 32 MPa and 10 points measures, as modal behaviour was better adjusted at low frequencies. The influence on the final results of the speed level difference will be evaluated later.

In elastic layer models, modal behaviour was more complex. A similar evolution of the mean square velocity values was observed in the experimental values and in the FEM models up until 1000 Hz, although comparisons were difficult due to the complexity of the response. The differences between own frequencies of the calculation models and those obtained experimentally were also observed by [42], with notable variations due to the difference in behaviour of the reduced mass in relation to the springs simulating the floating floor.

4. RESULTS AND DISCUSSION

Results on velocity level difference, $D_{\mathrm{v,ij}}$, in joints without an elastic layer, between thick plates joints and between thick plate-thin plate joints, are shown in Fig. 6. Three cases are represented: Experimental test, FEM model with tapping machine type excitation and FEM model with impact type excitation. For each case, the average results at three excitation points and with maximum and minimum values are shown, for third-octave frequency bands. A similar frequency relationship is observed in the experimental results and FEM models. Maximum and minimum values usually showed big differences compared to the mean value in both the experimental measurements and in the numerical calculations, especially in some frequency bands.

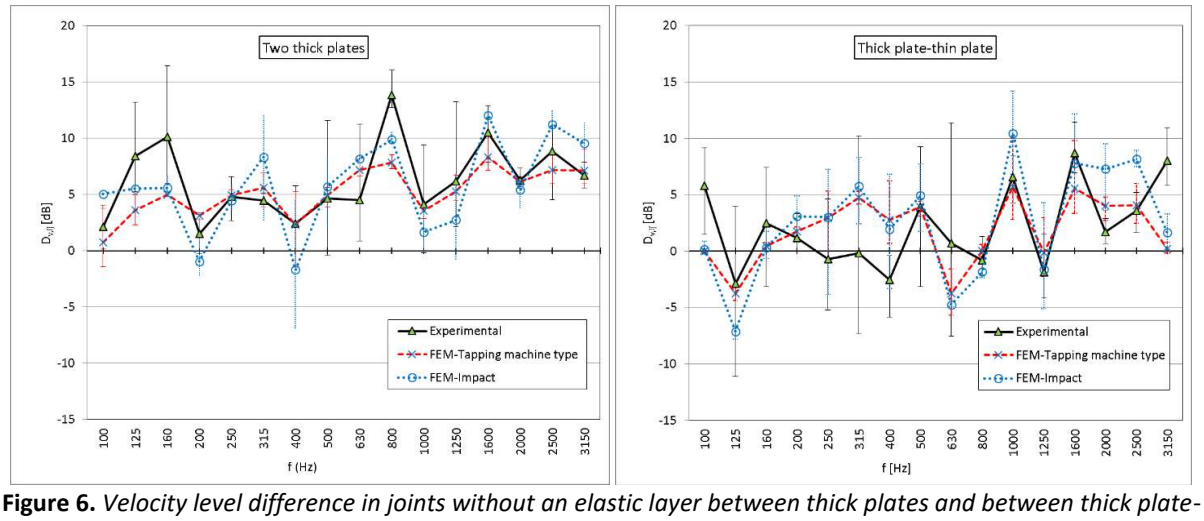

Figure 6. *Velocity level difference in joints without an elastic layer between thick plates and between thick plate-thin plate, impact type and tapping machine type excitation. Average of three excitation points and maximum and minimum values. ($D_{v,ij}$ - velocity level difference, f - frequency).*

In order to evaluate the predictive capacity of the FEM model without an elastic layer, calibrated with the F1 excitation, the weighted normalized impact sound pressure level, $L_{\mathrm{n,w}}$, according to EN ISO 717-2 [47] are shown in Fig. 7. In the case of the junction of thick plates without an elastic layer, almost all results showed differences smaller than 2 dB. The average experimental result was 14.7 dB and the average result for the FEM model and impact type excitation was 15.7 dB. In the case of

joining the thick and thin plates with no elastic layer, almost all the results, in the experimental measurements and in the FEM model, did not differ by more than 2 dB, being the average value 11.7 dB for the experimental measurements and 12.7 dB for the thick FEM model and impact type excitation.

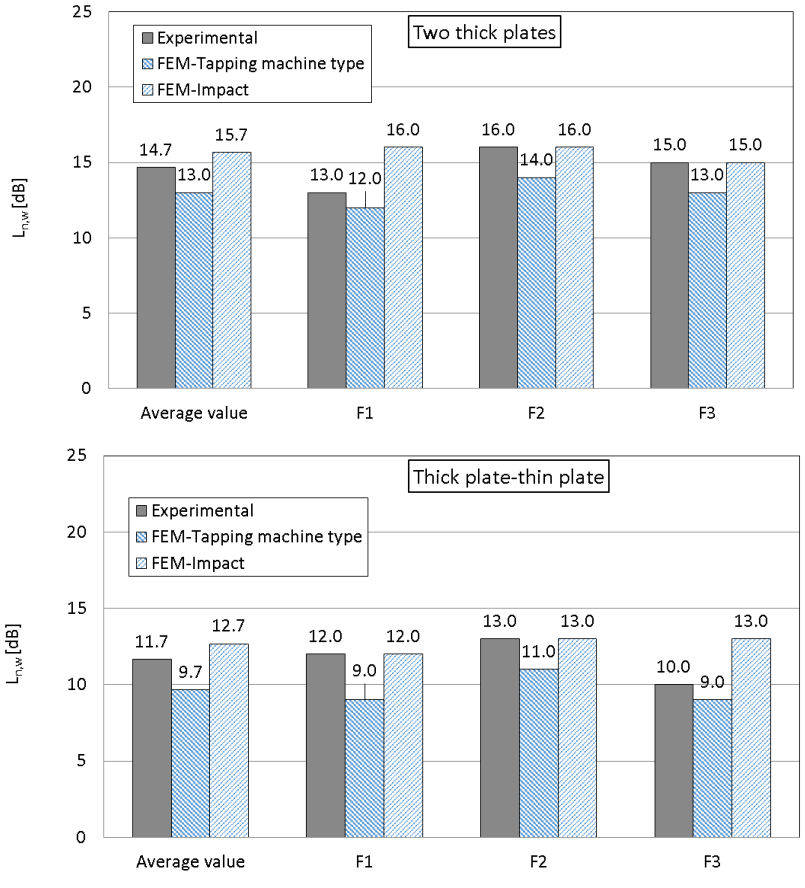

Figure 7. *Weighted normalized impact sound pressure level: average and values in the three excitation points. ($L_{n,w}$ - weighted normalized impact sound pressure level).*

For models with an elastic layer and floating floor, the results of the speed level difference, in the cases of thick plates and elastic layers, averaged and with maximum and minimum values, are shown in Fig. 8a and Fig. 8b. A similar relationship with frequency is observed in the experimental results and FEM models, using tapping machine type excitation to cover the desired frequency range.

Results of velocity level difference, in the case of thick and thin plate junction, averaged and with maximum and minimum values, are shown in Fig. 8c and Fig. 8d. A similar relationship with frequency is observed in experimental results and in FEM models, with somewhat lower values in the FEM model than in the experimental ones in the case of elastic layer 2.

In order to evaluate the predictive capacity of the FEM model with an elastic layer, values of the averaged frequency velocity level difference according to [47] in the case of thick plate junctions where a floating plate is used on the elastic layer, are shown in Fig. 9. The average result in experimental and FEM measurements showed a difference of around 1 dB, all values being comprised between 55 dB and 57 dB.

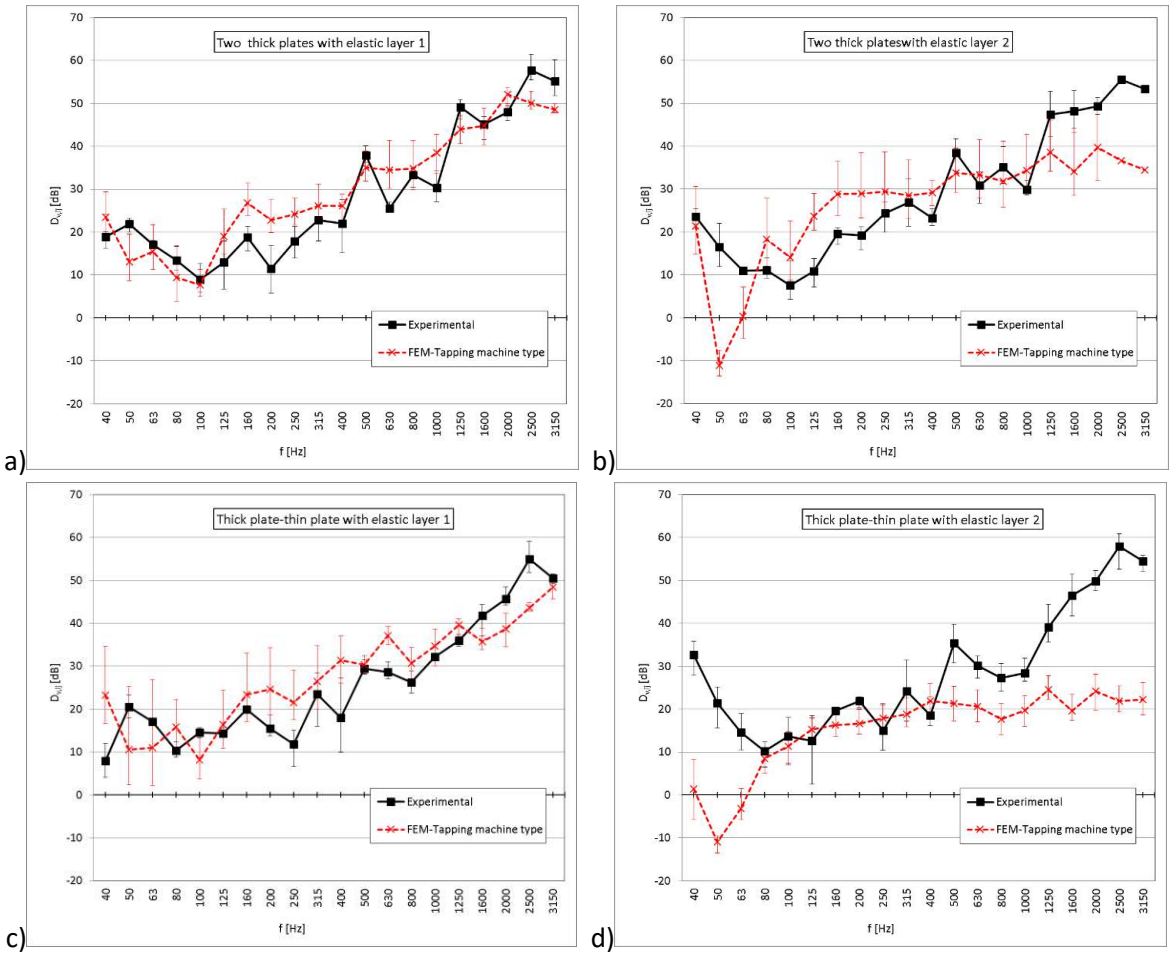

Figure 8. *Velocity level difference: two thick plates and a thick plate-thin plate. Elastic layer 1 and 2. Average of three excitations and maximum and minimum values. ($D_{v,ij}$ - velocity level difference, f – frequency).*

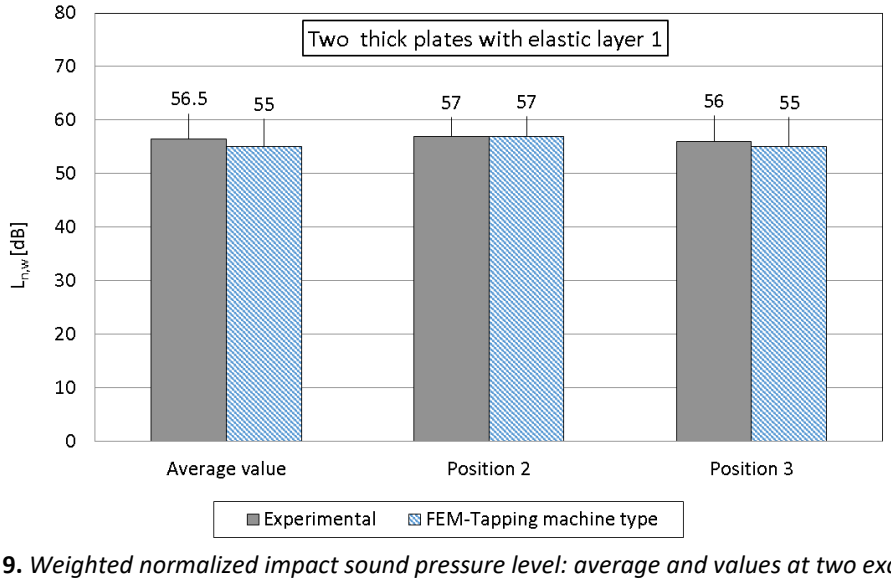

Figure 9. *Weighted normalized impact sound pressure level: average and values at two excitation points. ($L_{n,w}$ - weighted normalized impact sound pressure level).*

The values of the weighted normalized impact sound pressure level according to [47], for the different types of joints, are shown in Fig. 10. The experimental mean values and the FEM mean values, for joints without an elastic layer, differ by less than 2 dB. For elastic-layer joints, the difference between the mean values is between 1 dB and 14.3 dB, though in three out of four cases it was not greater than 7 dB.

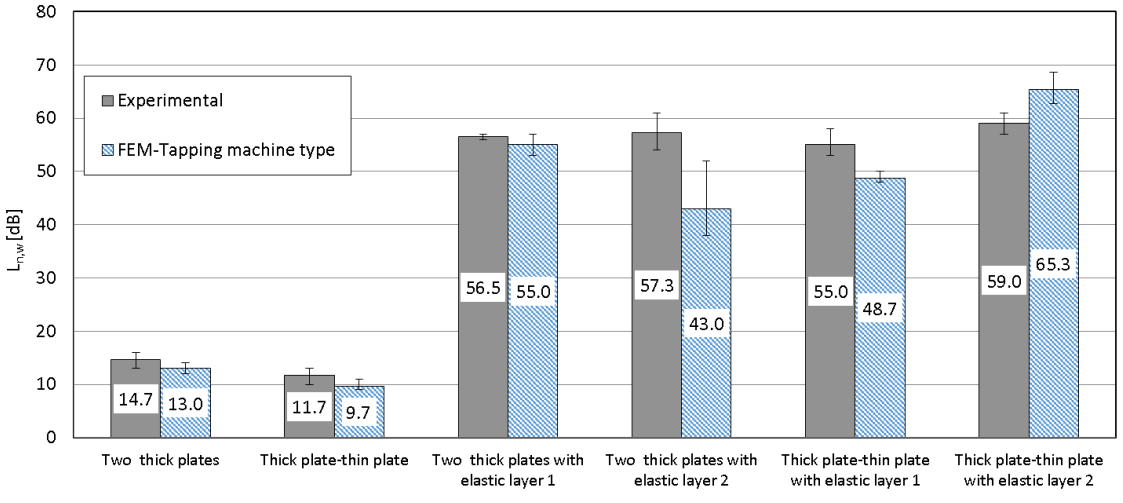

Figure 10. *Weighted normalized impact sound pressure level: average and maximum and minimum values. ($L_{n,w}$ - weighted normalized impact sound pressure level).*

5. CONCLUSIONS

The validation and calibration process allowed to make the adopted FEM model more reliable, by evaluating the differences with experimental measures and other FEM models. In this way, the most appropriate model and variability order of FEM models were determined based on the variable mesh size.

The use of randomly selected 10 points for measuring velocity produced satisfactory results in FEM models. The use of tapping machine type excitation enables to cover the desired frequency range.

The $D_{\mathrm{v,ij}}$ results for the models without an elastic layer showed a similar relationship with frequency in the experimental results and FEM models. The values averaged according to [47] showed similar results. In larger models, where the SEA can be applied with greater precision, it is expected that the FEM results achieve a better approximation to the experimental results.

In the elastic layer models 1 and 2, $D_{\mathrm{v,ij}}$ results had a similar relationship with frequency in the experimental results and in the FEM models. For the values averaged according to [47], experimental results and results of FEM models showed differences smaller than 7 dB in three of the four cases.

Worthy of note is that, even though the modal behaviour was complex in elastic layer models, and it was not possible to calibrate own frequencies very accurately, experimental and calculated results of the velocity level difference were fairly close. Therefore, it is recommended to validate FEM models using $D_{\mathrm{v,ij}}$.

As a result, FEM 2D models were developed and validated, obtaining results that were similar to those obtained through experimental measurements. This is a step forward in the use of virtual models in vibroacoustic study.

REFERENCES

[1] Hopkins, C. (2009). Experimental statistical energy analysis of coupled plates with wave conversion at the junction. Journal of Sound and Vibration, 322(1–2), 155–166. https://doi.org/http://dx.doi.org/10.1016/j.jsv.2008.10.025.

[2] Maluski, S. P. S., & Gibbs, B. M. (2000). Application of a finite-element model to low-frequency sound insulation in dwellings. The Journal of the Acoustical Society of America, 108(4), 1741–1751.

[3] Simmons, C. (1991). Structure-borne sound transmission through plate junctions and estimates of sea coupling loss factors using the finite element method. Journal of Sound and Vibration, 144(2), 215–227. https://doi.org/http://dx.doi.org/10.1016/0022-460X(91)90745-6.

[4] Mees, P., & Vermeir, O. (1993). Structure-Borne Sound Transmission at Elastically Connected Plates. Journal of Sound and Vibration, 166(1), 55–76. Retrieved from http://www.scopus.com/inward/record.url?eid=2-s2.0-0027912155&partnerID=40&md5=aa4c9d03e41a69fd5923f52476f05321.

[5] Steel, J. A., & Craik, R. J. M. (1994). Statistical Energy Analysis Of Structure-borne Sound Transmission By Finite Element Methods. Journal of Sound and Vibration, 178(4), 553–561. https://doi.org/http://dx.doi.org/10.1006/jsvi.1994.1503.

[6] Fredo, C. R. (1997). A SEA-like approach for the derivation of energy flow coefficients with a finite element model. Journal of Sound and Vibration, 199(4), 645–666. https://doi.org/http://dx.doi.org/10.1006/jsvi.1996.0634.

[7] Mace, B. R., & Shorter, P. J. (2000). Energy flow models from finite element analysis. Journal of Sound and Vibration, 233(3), 369–389. https://doi.org/http://dx.doi.org/10.1006/jsvi.1999.2812.

[8] Wang, Z. H., Xing, J. T., & Price, W. G. (2002). An investigation of power flow characteristics of L-shaped plates adopting a substructure approach. Journal of Sound and Vibration, 250(4), 627–648. https://doi.org/http://dx.doi.org/10.1006/jsvi.2001.3956.

[9] Hopkins, C. (2003a). Vibration transmission between coupled plates using finite element methods and statistical energy analysis. Part 1: Comparison of measured and predicted data for masonry walls with and without apertures. Applied Acoustics, 64(10), 955–973. https://doi.org/10.1016/S0003-682X(03)00062-8.

[10] Hopkins, C. (2003b). Vibration transmission between coupled plates using finite element methods and statistical energy analysis. Part 2: The effect of window apertures in masonry flanking walls. Applied Acoustics, 64(10), 975–997. https://doi.org/10.1016/S0003-682X(03)00063-X.

[11] EN 12354-1:2000. (2000). Building acoustics – Estimation of acoustic performance of buildings from the performance of elements. Part 1: Airborne sound insulation between rooms.

[12] Craik, R. J. M., Bosmans, I., Cabos, C., Heron, K. H., Sarradj, E., Steel, J. A., & Vermeir, G. (2004). Structural transmission at line junctions: a benchmarking exercise. Journal of Sound and Vibration, 272(3–5), 1086–1096. https://doi.org/http://dx.doi.org/10.1016/j.jsv.2003.07.011.

[13] Bochniak, W., & Cieslik, J. (2005). Uncertainty in vibration energy flow analysis. Archives of Acoustics, 30(4), 451–463. Retrieved from http://www.scopus.com/inward/record.url?eid=2-s2.0-30344435332&partnerID=40&md5=bd6e5db27fa4b674031166a4b43dba5c.

[14] Iwaniec, M. (2006). Application of genetic algorithms to the evaluation of the fundamental frequency of stiffened plates. Archives of Acoustics, 31(3), 335–346. Retrieved from http://www.scopus.com/inward/record.url?eid=2-s2.0-33748804957&partnerID=40&md5=e5382b04b868b6599160efa9449d541b.

[15] Clasen, D., & Langer, S. (2007). Finite element approach for flanking transmission in building acoustics. Building Acoustics, 14(1), 1–14. Retrieved from http://www.scopus.com/inward/record.url?eid=2-s2.0-80054806668&partnerID=40&md5=c864e8498a38f29ff9c2100ba855ea95.

[16] Du, J., Li, W. L., Liu, Z., Yang, T., & Jin, G. (2011). Free vibration of two elastically coupled rectangular plates with uniform elastic boundary restraints. Journal of Sound and Vibration, 330(4), 788–804. https://doi.org/http://dx.doi.org/10.1016/j.jsv.2010.08.044.

[17] Ramis, J., Segovia, E., Alba, J., Carbajo, J., & Godinho, L. (2012). Numerical evaluation of the vibration reduction index for structural joints. Archives of Acoustics, 37(2), 189–197.

[18] Wang, X., & Hopkins, C. (2014). Application of SEA and Advanced SEA to structure-borne sound transmission on a rectangular beam framework. In 21st International Congress on Sound and Vibration (pp. 13–17).

[19] Wawrzynowicz, A., Krzaczek, M., & Tejchman, J. (2014). Experiments and FE analyses on airborne sound properties of composite structural insulated panels. Archives of Acoustics, 39(3), 351–364. Retrieved from http://www.scopus.com/inward/record.url?eid=2-s2.0-84926616910&partnerID=40&md5=a665d43279a9029cf631a0e2be6af75d.

[20] Shi, S., Jin, G., & Chen, M. (2014). The modeling and free vibration analysis of coupled plates of various types. In D. C. D. L. M. T. B. N. Davy J. Burgess M. (Ed.), INTERNOISE 2014 - 43rd International Congress on Noise Control Engineering: Improving the World Through Noise Control. Australian Acoustical Society. Retrieved from https://www.scopus.com/inward/record.uri?eid=2-s2.0-84923625032&partnerID=40&md5=3251e2b43dc7fdd3e6352063467e2b2a.

[21] Wang, J.-F. (2014). Vibration Analysis of Moderately Thick Coupled Rectangular Plates. Proceedings of the 2014 International Conference on Mechanics and Civil Engineering, 7, 272–276. Retrieved from %3CGo.

[22] Poblet-Puig, J., & Guigou-Carter, C. (2015). Using spectral finite elements for parametric analysis of the vibration reduction index of heavy junctions oriented to flanking transmissions and EN-12354 prediction method. Applied Acoustics, 99(0), 8–23. https://doi.org/http://dx.doi.org/10.1016/j.apacoust.2015.03.025.

[23] Hopkins, C., Crispin, C., Poblet-Puig, J., & Guigou-Carter, C. (2016). Regression curves for vibration transmission across junctions of heavyweight walls and floors based on finite element methods

and wave theory. Applied Acoustics, 113, 7–21. https://doi.org/http://dx.doi.org/10.1016/j.apacoust.2016.06.002.

[24] Wilson, E. L. (2002). Three-dimensional static and dynamic analysis of structures: a physical approach with emphasis on earthquake engineering (Vol. 3). Berkeley: Computers and structures.

[25] Carson II, J. S. (2002). Model verification and validation. In Winter Simulation Conference Proceedings (Vol. 1, pp. 52–58). Retrieved from http://www.scopus.com/inward/record.url?eid=2-s2.0-0036928328&partnerID=40&md5=cb1f4e42e649d4ed80612216ebc1f0f9.

[26] Thacker, B. H., Doebling, S. W., Hemez, F. M., Anderson, M. C., Pepin, J. E., & Rodriguez, E. A. (2004). Concepts of model verification and validation. Los Alamos National Lab., Los Alamos, NM (US).

[27] Babuska, I., & Oden, J. T. (2004). Verification and validation in computational engineering and science: Basic concepts. Computer Methods in Applied Mechanics and Engineering, 193(36–38), 4057–4066. Retrieved from http://www.scopus.com/inward/record.url?eid=2-s2.0-4344712048&partnerID=40&md5=6e3e07950e831b8d7eddbfbe84c57f2c.

[28] Oberkampf, W. L., & Trucano, T. G. (2008). Verification and validation benchmarks. Nuclear Engineering and Design, 238(3), 716–743. https://doi.org/10.1016/j.nucengdes.2007.02.032.

[29] Tian, W., Yao, L., & Li, L. (2017). A Coupled Smoothed Finite Element-Boundary Element Method for Structural-Acoustic Analysis of Shell. Archives of Acoustics, 42(1), 49–59. https://doi.org/10.1515/aoa-2017-0006.

[30] Gerretsen, E. (1994). European developments in prediction models for building acoustics. Acta Acustica, 2(3), 205–214.

[31] EN ISO 10848-1:2006. (2006). Acoustics – Laboratory measurement of the flanking transmission of airborne and impact sound between adjoining rooms – Part 1: Frame document.

[32] Gerretsen, E., & Nightingale, T. R. T. (1999). Prediction models in building acoustics: Introduction to the special session at Forum Acusticum 1999 in Berlin. Building Acoustics, 6(3), 151–158. Retrieved from http://www.scopus.com/inward/record.url?eid=2-s2.0-84864689913&partnerID=40&md5=ea66a868876b8869384a94bffa00c0ad.

[33] Gerretsen, E. (2005). Development and use of prediction models in building acoustics as in EN 12354. In Forum Acusticum Budapest 2005: 4th European Congress on Acustics (pp. 1893–1899). Retrieved from http://www.scopus.com/inward/record.url?eid=2-s2.0-84864625499&partnerID=40&md5=a1b57ec07e02607cbd6df6eaf44b5cd9.

[34] Gerretsen, E. (2008). Prediction models for building performance - European need and world wide use. In Proceedings - European Conference on Noise Control (pp. 1663–1667). Retrieved from http://www.scopus.com/inward/record.url?eid=2-s2.0-84874891657&partnerID=40&md5=c4b9fba935edc3428ba3acce2c1a2860.

[35] Gerretsen, E. (2009). The development of the EN 12354 series: 1989-2009. In 8th European Conference on Noise Control 2009, EURONOISE 2009 - Proceedings of the Institute of Acoustics (Vol. 31). Retrieved from http://www.scopus.com/inward/record.url?eid=2-s2.0-84864701500&partnerID=40&md5=1a6f34a2097f36b734856411262f9324.

[36] Guyader, J. L., Boisson, C., & Lesueur, C. (1982). Energy transmission in finite coupled plates, part I: Theory. Journal of Sound and Vibration, 81(1), 81–92. https://doi.org/http://dx.doi.org/10.1016/0022-460X(82)90178-X.

[37] Boisson, C., Guyader, J. L., Millot, P., & Lesueur, C. (1982). Energy transmission in finite coupled plates, part II: Application to an L shaped structure. Journal of Sound and Vibration, 81(1), 93–105. https://doi.org/http://dx.doi.org/10.1016/0022-460X(82)90179-1.

[38] Torres, J., Cárdenas, W., Carbajo, J., Segovia, E., & Ramis, J. (2012). Estudio de la radiación en vigas utilizando la técnicas de medición de holografía de campo cercano. In VIII Congreso Ibero-americano de acústica.

[39] Molina, P., Torres, J., Segovia, E., & Ramis, J. (2014). Estudio de la transmisión de las vibraciones usando modelos a tamaño reducido. In Tecniacústica 2014. Murcia.

[40] Huang, H. C., & Hinton, E. (1986). A new nine node degenerated shell element with enhanced membrane and shear interpolation. International Journal for Numerical Methods in Engineering, 22(1), 73–92.

[41] Hughes, T. J. R., & Hinton, E. (1986). Finite element methods for plate and shell structures (Vol. 1). Pineridge Press International.

[42] Cho, T. (2013). Vibro-acoustic characteristics of floating floor system: The influence of frequency-matched resonance on low frequency impact sound. Journal of Sound and Vibration, 332(1), 33–42. https://doi.org/http://dx.doi.org/10.1016/j.jsv.2012.07.047.

[43] Magdaleno, J. (2015). Simulación numérica de la transmisión indirecta estructural y de la transmisión del ruido de impactos en edificios. Universidad de Valladolid. Retrieved from http://uvadoc.uva.es/handle/10324/16297.

[44] Mottershead, J. E., & Friswell, M. I. (1993). Model updating in structural dynamics: A survey. Journal of Sound and Vibration, 167(2), 347–375. Retrieved from http://www.scopus.com/inward/record.url?eid=2-s2.0-0027683685&partnerID=40&md5=060277b5c9f8bc0ac38fc3dd61bf18bf.

[45] Mottershead, J. E., Link, M., & Friswell, M. I. (2011). The sensitivity method in finite element model updating: A tutorial. Mechanical Systems and Signal Processing, 25(7), 2275–2296. https://doi.org/http://dx.doi.org/10.1016/j.ymssp.2010.10.012.

[46] Hopkins, C. (2007). Sound insulation. Elsevier / Butterworth-Heinemann. Retrieved from http://almena.uva.es/search~S1*spi?/tsound+insulation/tsound+insulation/1,1,1,B/frameset&FF=tsound+insulation&1,1,?save=b1634652.

[47] EN ISO 717-2:2013. (2013). Acoustics – Rating of sound insulation in buildings and of building elements – Part 2: Impact sound insulation.